



# Strength–ductility combination of fine-grained magnesium alloy with high deformation twin density

F. Zhao <sup>a,\*</sup>, T. Suo <sup>b</sup>, B. Chen <sup>c</sup>, Y.L. Li <sup>b</sup>

HPSTAR  
783-2019



<sup>a</sup> Institute for Advanced Study, Chengdu University, Chengdu 610106, China

<sup>b</sup> School of Aeronautics, Northwestern Polytechnical University, Xi'an 710072, China

<sup>c</sup> Center for High Pressure Science and Technology Advanced Research, Pudong, Shanghai 201203, China

## ARTICLE INFO

### Article history:

Received 28 November 2018

Received in revised form

20 May 2019

Accepted 21 May 2019

Available online 23 May 2019

### Keywords:

AZ31 Mg alloy

Deformation twins

Mechanical behaviors

Grain refinement

Microstructure evolution

## ABSTRACT

The objective of present study is to determine the effects of grain size and deformation twin density on mechanical behaviors linked to microstructure evolution of AZ31 magnesium (Mg) alloy. The AZ31 Mg alloy was processed by warm severe plastic deformation method and followed by dynamic compression (strain rate  $\sim 1 \times 10^3 \text{ s}^{-1}$ , plastic strain  $\sim 10\%$ ). Uniaxial tensile experiments at room temperature have revealed that AZ31 Mg alloy is exhibited enhanced strength with grain refinement and high deformation twin density. The improved strength of AZ31 Mg alloy is attributed to the hindering effect of increasing grain boundaries (GBs) and twin boundaries (TBs) on dislocation motion, thereby making plastic deformation more difficult. As a result, the large reduction in ductility has been found for fine grained AZ31 Mg alloy (grain size is about 2–3  $\mu\text{m}$ ). But with increasing deformation twin density after dynamic compression (especially in fine grained samples), the obvious ductility enhancement has been found in both coarse grained and fine grained AZ31 Mg alloy. With mechanical behaviors properly described, both strength and ductility can be simultaneously achieved in fine grained and high twin density AZ31 Mg alloy.

© 2019 Elsevier B.V. All rights reserved.

## 1. Introduction

Magnesium alloys, the lightest structural metals, have been increasingly applied in many industries such as automotive & transportation, electronics, and aerospace & defense [1–3]. However, the poor mechanical properties, such as low strength and ductility, limit their extended applications and need further development [4,5]. At ambient temperature, due to their hexagonal close packed (h.c.p) crystalline structure, Mg alloys deform primarily through basal slips, which are activated through the lowest critical resolved shear stress (CRSS) than other slip systems and deformation twins [6]. Besides basal slip, it is the activation of  $\langle c+a \rangle$  slip on second order pyramidal planes, but the pyramidal  $\langle c+a \rangle$  dislocations always undergo a rapid transition to an immobile structure at room temperature [7]. Moreover, the activation of non-basal slip systems is only at high stress regions like GBs and TBs at room temperature [8].

Grain refinement and pre-twinning are important and

frequently-used method for improving mechanical behaviors of Mg alloys [9,10]. Severe plastic deformation methods have always been used to enhance the strength of Mg alloy by microstructure refinement [11–13]. Through grain refinement, the strength of Mg alloys also could be effectively improved, but the large reduction in ductility has been found for fine grained Mg alloy [14]. Fatemi-Varzaneh and Zarei-Hanzaki introduce a novel severe plastic deformation method calls accumulative back extrusion (ABE) to fabricate ultrafine grained AZ31 Mg alloy, which exhibits large ductility at room temperature [15]. Although a number of studies have been proposed to describe the grain refinement effect on ductility [16], as summarized above, the role of fine grained structure on improving the formability or ductility of Mg alloys is still mixed and even controversial. The underlying micro-mechanisms are still need to be comprehensively clarified.

Moreover, deformation twin also is a important deformation mechanism of Mg alloys during plastic deformation [17]. Besides dislocation nucleation and motion on basal slip,  $\{10\bar{1}2\}$  extension twin is another pronounced deformation mode due to its low CRSS [18]. The extension twins have always been formed during the early stage of plastic deformation [19]. High twin density can largely

\* Corresponding author.

E-mail address: [zhaofeng@cdu.edu.cn](mailto:zhaofeng@cdu.edu.cn) (F. Zhao).

improve the ductility of many h.c.p materials by activating more slip systems and providing more needed strain along the *c*-axis [20]. Armsrong and Worthington have suggest that twinning is easier nucleation in fine grained Mg alloy, which have high stress concentrations within local regions of the microstructure whereas slip is more uniform [21]. So, one potential method for improving the ductility of Mg alloys is increase the deformation twin density in fine grained Mg alloy at room temperature.

With the aim of improving the strength and ductility of Mg alloys by grain refinement and high deformation twin density, we examined the mechanical behaviors of AZ31 alloy with different grain size and twin density. Also, microstructure characterizations were carried out to investigate the effects of GBs and TBs on plastic deformation.

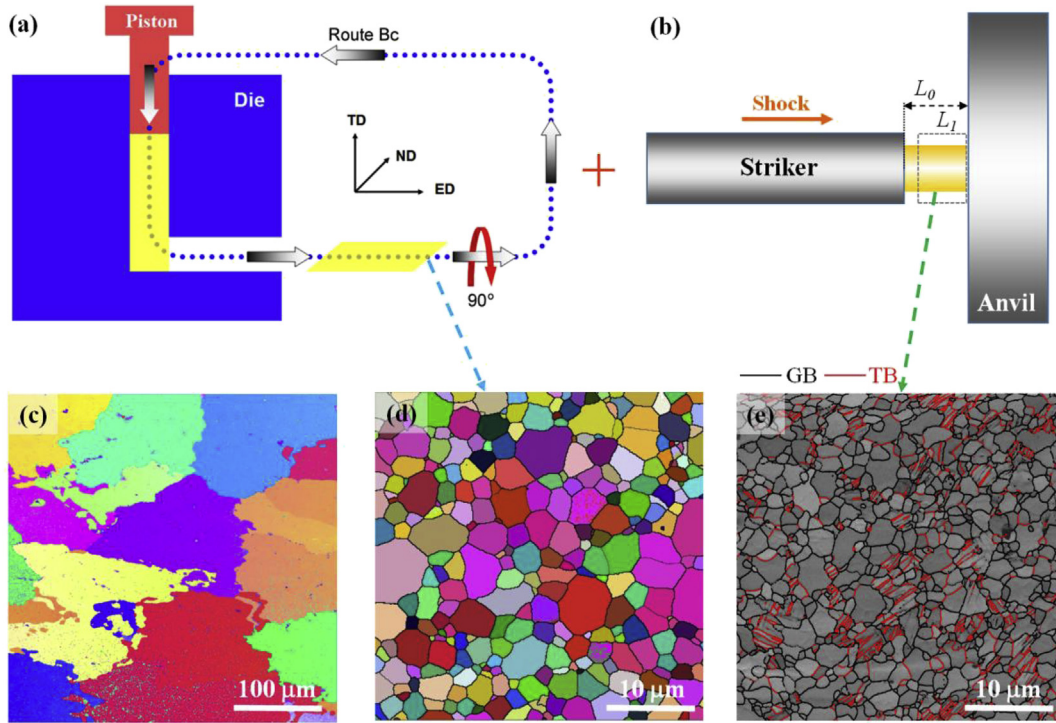


**Fig. 1.** Schematic diagram of the equal channel angular pressing (ECAP) setup (a) and dynamic compression facility (b). The microstructure of (c) as-received, (d) ECAPed and (e) ECAPed and dynamic-compressed AZ31 Mg alloy.

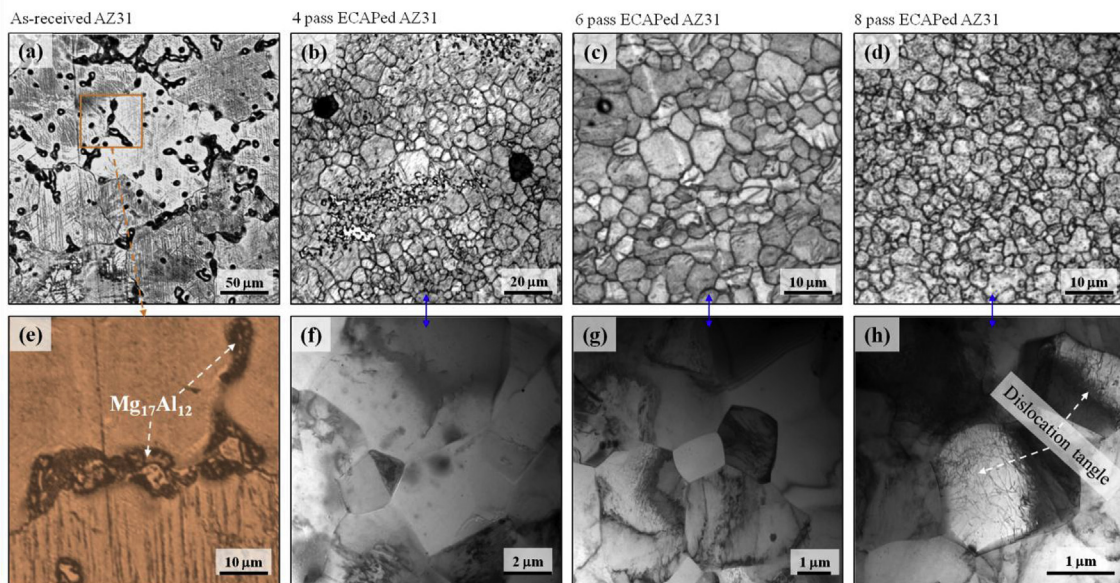


**Fig. 2.** Microstructure of the AZ31 alloy (a)–(d) in, from the left, as-cast and as-processed conditions through ECAP for 4, 6 and 8 pass, and corresponding (e) second phase and (f)–(h) TEM characterizations of 4, 6 and 8 pass of ECAPed AZ31 alloy.

## 2. Experimental and methods

### 2.1. Thermo-sever plastic deformation and shock compression

Herein, the as-cast AZ31 (mass: Al 3.0%, Zn 1.0%, Mn 0.4%, Mg balance) Mg alloy ingot was used as the initial material in this study. The grain size of as-received AZ31 sample was measured to be  $150 \pm 5 \mu\text{m}$  (see Fig. 1(c)). The work pieces with dimensions of  $60 \times 10 \times 10 \text{ mm}^3$  were cut from the as-received AZ31 for processing by equal channel angular pressing (ECAP). The ECAP die with inner channel angle  $90^\circ$  and outer arc angle  $0^\circ$  was used, as shown in Fig. 1 (a). During ECAP process, the die set was heated with four heating pillars and a thermocouple placed exactly near the channel corner was used to monitor and control the process temperature. The ECAP process was carried out following route B<sub>c</sub>, in which billet was rotated by  $90^\circ$  in the same rotational direction

between each pass. The pressing speed was kept  $\sim 15 \text{ mm}$  per minute. Prior to each pass, the billet was well lubricated and pre-heated to reach the required processing temperature for 10 min. The first pass was conducted at  $300 \pm 10^\circ\text{C}$ , and then, deformation temperature was gradually lowered in steps after each pass. The final 8 pass ECAP process was conducted at  $230 \pm 10^\circ\text{C}$ . After each pass, the average cumulative strain in the deformed billet was about 1.15 according to the theory calculation or FEM simulations [22,23]. After ECAP processed, the grain size are largely reduced to several micrometers and without any obvious deformation twins, as show in Fig. 1(d).

After ECAP processed, the 4, 6 and 8 pass ECAPed samples were performed by dynamic compression for introducing high density of deformation twin. The dynamic compression facility is shown schematically in Fig. 1(b). Compressive samples were subjected to shock compression on a fixed anvil to ensure that samples

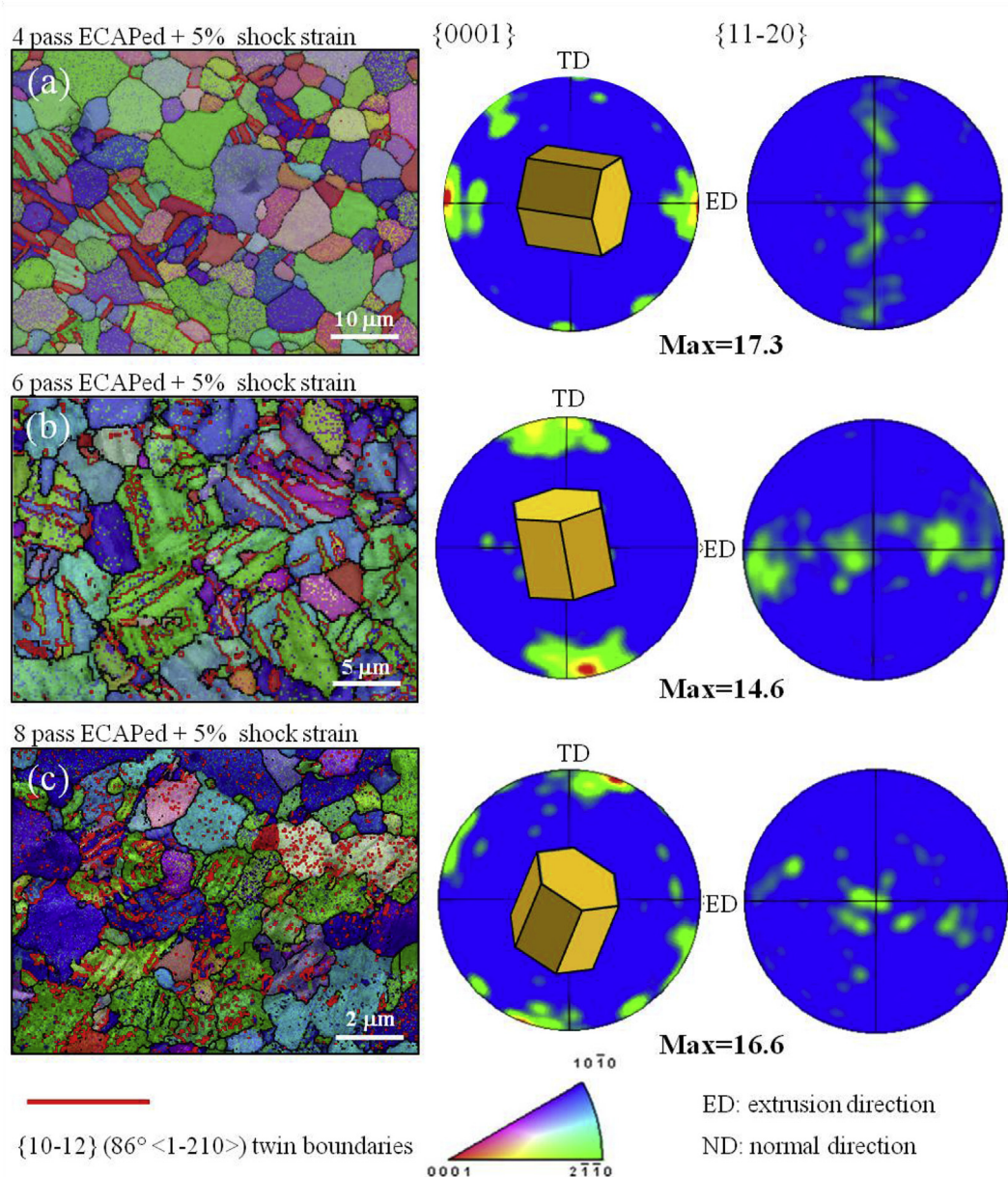


Fig. 3. EBSD inverse pole figure maps and  $\{0001\}$ ,  $\{11\bar{2}0\}$  pole figure maps of (a) 4pass ECAPed + 5% shock strain, (b) 6pass ECAPed + 5% shock strain and (c) 8pass ECAPed + 5% shock strain of AZ31 alloy.

deformed at high strain rate. During dynamic compression, high pressure air gun were used to press the striker, which then pressing the AZ31 samples. The pressing velocity was about 10 m/s, which measured by magnet induction system. The strain rate applied in shock compression was estimated to be  $1 \times 10^3 \text{ s}^{-1}$ . The compressive strain is defined as  $\varepsilon = \ln(L_0/L_f)$ , where  $L_0$  and  $L_f$  are the initial and final thickness of deformed samples. After dynamic compression, many twin bands identified as  $\{10\bar{1}2\}$  extension twins were discerned in the AZ31 samples. In order to get rid of residual stress and remove high density dislocation structures, the AZ31 samples were annealed at 200 °C for 30 min after dynamic compression.

## 2.2. Microstructure investigation

In order to investigate the microstructure evolution after ECAP and dynamic compression processes, microstructure characterizations were conducted on the as-received, multi-pass ECAPed, and shock compressed samples by using optical microscopy (OM), electron back-scattered diffraction (EBSD) and transmission electron microscopy (TEM). EBSD mapping using a step size of 1  $\mu\text{m}$  was performed on an FEI quanta 450 scanning electron microscope (SEM) with an HKL-EBSD system. TEM specimens were cut from deformed and tensile tested samples in a plane containing the normal and extrusion or tension direction. TEM characterizations were conducted by using Philips CM12 TEM at an accelerating voltage of

120 kV. After tensile tests, the fracture surface morphology was characterized by SEM.

## 2.3. Uniaxial tensile test

Mechanical properties were examined by uniaxial tensile testing to evaluate the effect of grain refinement and high density of deformation twin on mechanical behaviors in the AZ31 Mg alloy. Uniaxial tensile tests were carried out using an electronic universal testing machine at room temperature at a constant strain rate of  $1.0 \times 10^{-3} \text{ s}^{-1}$ , and the tension direction was parallel to the ECAP extrusion and dynamic compression direction.

## 3. Results

### 3.1. Microstructural evolution

OM, TEM and EBSD characterizations of as-received, ECAPed and dynamic compressed AZ31 samples are shown in Figs. 2 and 3 respectively. Fig. 2 shows the representative OM (a)–(e) and TEM microstructures (f)–(h) of the AZ31 Mg alloy in, from the left, as-cast and 4, 6 and 8 ECAP processed conditions. After ECAP processed, the OM and TEM micrographs were all taken at the surfaces which perpendicular to the extrusion direction. Fig. 2(a) shows the initial

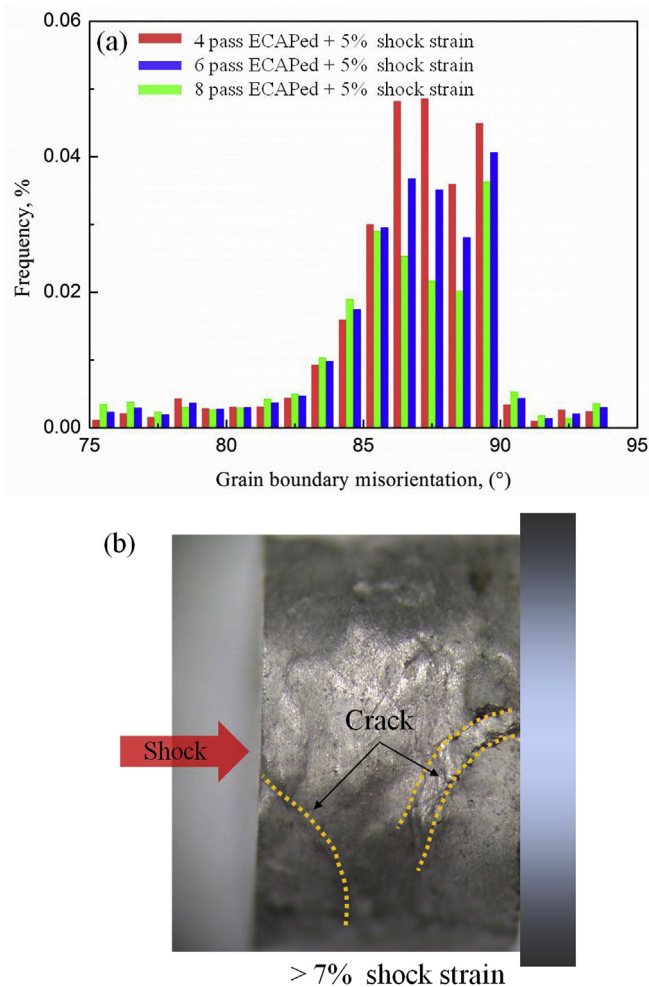


Fig. 4. (a) Misorientation distributions in various processed AZ31 alloy and (b) the cracks nucleation and propagation during dynamic-compressed process.

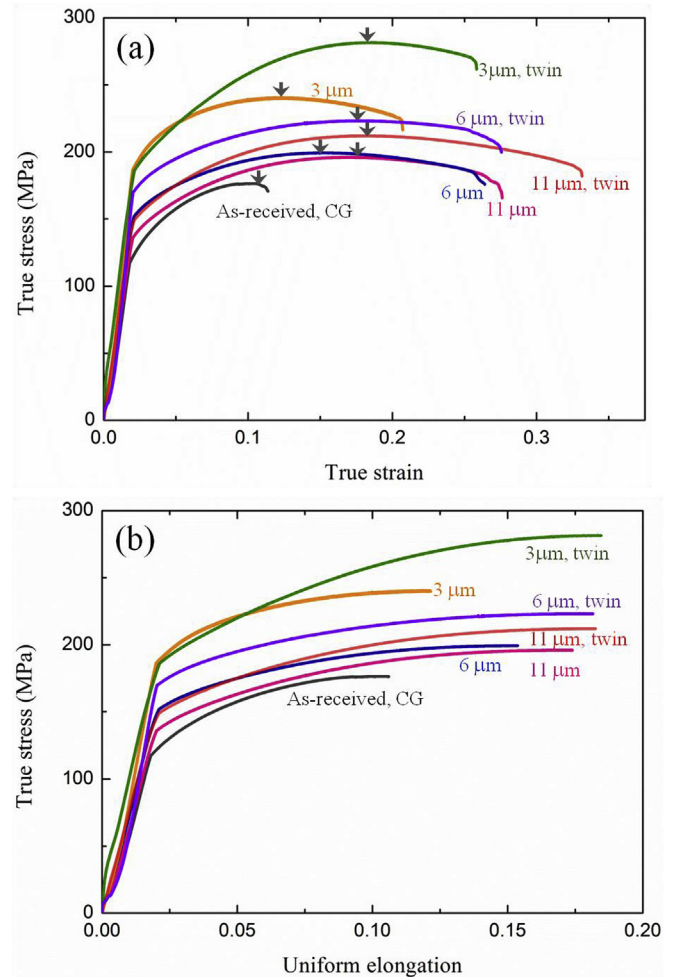


Fig. 5. The mechanical behaviors of AZ31 alloy with different microstructures, (a) the tensile true stress – true strain curves, (b) the tensile true stress – uniform elongation curves.

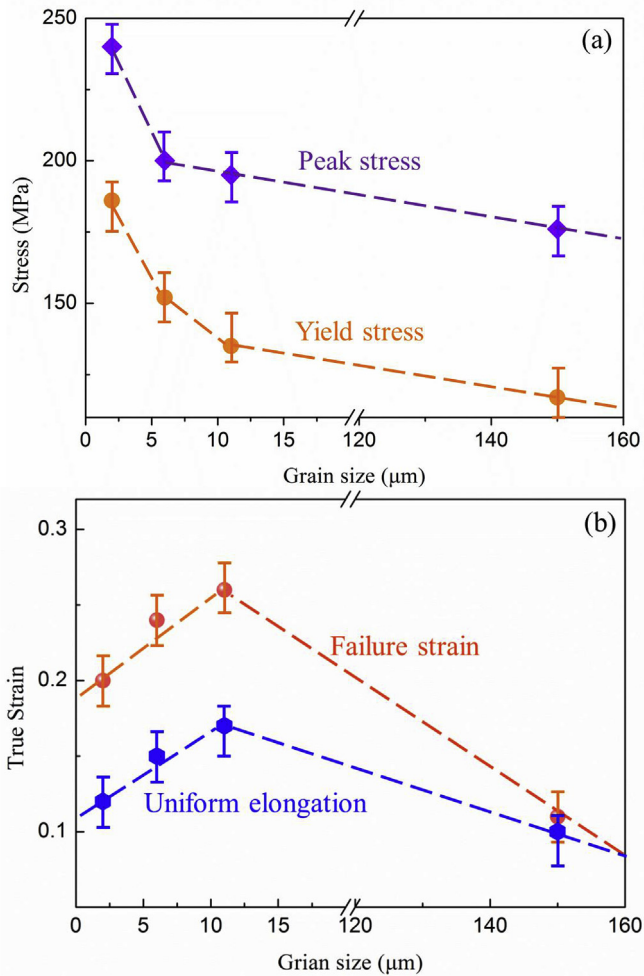


Fig. 6. Grain size effect on (a) yield and peak stress, (b) uniform elongation and failure strain of AZ31 alloy at room temperature.

microstructure of as-cast AZ31 sample, the average grain size is about  $150 \pm 5 \mu\text{m}$ , and typical second phase  $\text{Mg}_{17}\text{Al}_{12}$  can be seen near the GBs, as shown in Fig. 2(e). It is apparent from Fig. 2, effective grain refinement is achieved after each pass of ECAP process in AZ31 samples. The AZ31 samples are refined from an as-cast condition with initial grain size of  $\sim 150 \mu\text{m}$ – $\sim 3 \mu\text{m}$  after 8 pass ECAP processed, see in Fig. 2(d) and (e). After 4pass and 6pass ECAP processed, there are several large grains and without achieving microstructural homogeneity in AZ31 samples. The average grain size is about  $\sim 11 \mu\text{m}$  and  $\sim 6 \mu\text{m}$  respectively, as shown in Fig. 2(b), (c), (f) and (g). Overall, after multi-pass ECAP processed, grain refinement and high dislocation density structures are visible and without any obvious deformation twins (the twin density is less than 0.2%).

It is known that the CRSS of  $\langle c+a \rangle$  second-order pyramidal slips is much higher than extension twinning at low temperature or high strain rate loading conditions [24–26]. In order to introduce high density of deformation twin in AZ31 Mg alloy, the dynamic compression with limiting 5% compressive strain were performed in 4, 6 and 8 pass ECAPed AZ31 samples. The microstructure of dynamic compressed samples has been investigated by EBSD and the results are shown in Fig. 3. It can be observed that many deformation twins have been activated after dynamic compression. All the deformation twins are confirmed to be  $\{10\bar{1}2\}\langle 86^\circ \langle 1\bar{2}10 \rangle$  extension twins and without contraction twins. Due to the

difference in initial grain size, twin density increases with grain size reducing. Furthermore, the pole figures of dynamic compressed samples are shown in Fig. 3(a), (b) and (c), for 4 pass ECAPed with 5% dynamic compressive strain sample,  $\{0001\}$  pole figure represents that the  $c$ -axis rotated from normal direction (ND) to extrusion direction (ED) and contributed to the ED component. In 6 and 8 pass ECAPed with 5% dynamic compressive samples, a transverse direction (TD) component appeared in the  $\{0001\}$  pole figure along with ED component, which has a slightly smaller intensity than ED component. Moreover, the basal component became very small for all samples.

Fig. 4(a) shows the quantitative analysis of the change in the orientation distribution with dynamic compressed AZ31 samples with different initial grain size. A peak around  $\sim 86^\circ$  in Fig. 4(a) further confirms the presence of  $\{10\bar{1}2\}\langle 86^\circ \langle 1\bar{2}10 \rangle$  extension twins in a large number of grains and the tiny differences in orientation are caused by high density dislocation structures, which can be found in the vicinity near TBs [27]. The orientation distribution also proves that twin density increasing with grain size reduction. In our works, there is no any obvious crack in samples after ECAP process. During dynamic compressed process, for acquiring more TBs in AZ31 samples, we increased the compressive strain above 5%, and found some obvious cracks occurring in AZ31 samples at room temperature, as shown in Fig. 4(b). In order to exclude the crack effect on mechanical behaviors of AZ31 samples, all samples were dynamic compressed at 5% strain.

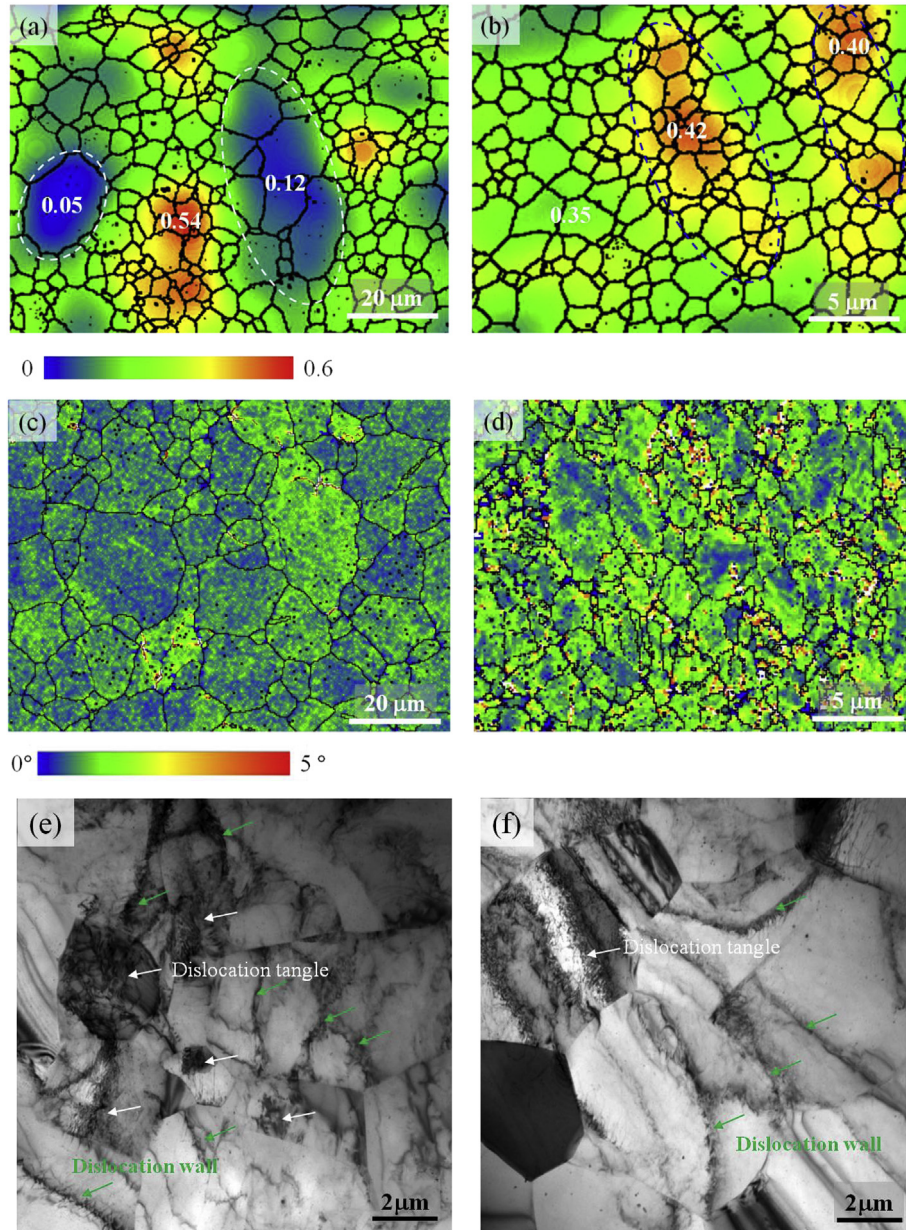
### 3.2. Mechanical behaviors

Fig. 5(a), (b) show the tensile true stress-true strain curves of AZ31 samples with different microstructure under the strain rate of  $1.0 \times 10^{-3} \text{ s}^{-1}$  at room temperature. Overall, after grain refinement and pre-twinning, the yield strength shows strong grain size and twin density dependence. The true stress-true strain curves demonstrate that grain size and pre-twinning has great enhancement on strength and ductility of AZ31 Mg alloy. With grain size reduction, the sample with average grain size  $3 \mu\text{m}$  (8 pass ECAPed AZ31 sample) exhibits the highest yield strength ( $\sim 185 \text{ MPa}$ ). And the sample with average grain size  $11 \mu\text{m}$  and pre-twinning shows largest tensile strain, which is about 34%. Fig. 5(b) shows the relationship between uniform elongation and true stress. Interestingly, the obvious enhancement of uniform elongation of AZ31 Mg alloy is occurred in samples after dynamic compressed (grain size: 11, 6 and  $3 \mu\text{m}$  with pre-twinning). And, note that the uniform elongation is as large as 18%. The true stress-true strain curves performed at room temperature also show that the pre-twinning samples have strong strain hardening capacity, which also contributes to the large uniform elongation.

## 4. Discussion

### 4.1. Grain size effect on the tensile plastic deformation and twin density

It was demonstrated that Mg alloys, which usually have low strength, could be strengthened by grain refinement. Their tensile yield and peak strength could be remarkable enhancement by grain refinement, as shown in Fig. 6(a). As the grain size reduced to  $3 \mu\text{m}$ , the yield strength is as high as 175 MPa. The high strength in AZ31 Mg alloy is caused by grain refinement, which increases the impeding effect on dislocation motion during plastic deformation. Also, after the ECAP processed, AZ31 Mg alloys always show a strong texture effect, which comes from the basal plane of most grains is parallel to shear direction or about  $45^\circ$  to the pressing



**Fig. 7.** The micro-strain maps, Kernel average misorientation maps and TEM images of bimodal microstructures (a), (c) and (e); and corresponding fine grained microstructures (b), (d) and (f) AZ31 Mg alloy after tension tests.

direction during severe plastic deformation [28]. As our tension tests have been performed in extrusion direction, so the initial texture and basal dislocation slip results in the lower strength but higher ductility of the fine grained AZ31 Mg alloy (texture softening effect). Therefore, the high yield and peak strength in fine grained AZ31 specimens is only caused by fine grains strengthening.

Conventionally, grain refinement in the AZ31 alloy is expected to contribute to the improvement of ductility, as shown in Fig. 6(b). During tensile plastic deformation, the AZ31 samples with average grain size of 11 μm exhibit the largest uniform elongation (17%) and failure strain (26%). Even though the grain size of 8 pass ECAPed AZ31 samples were greatly refined to 3 μm, their ductility and failure strain was reduced to 12% and 20%, respectively.

From the direct microstructural observations (Fig. 2(b), (c) and (d)), the grain refinement of AZ31 samples with average grain size of 11 μm was not uniform. The majority of the grains were in the

fine grain range (2–5 μm), and still there was a minority volume fraction of coarse grains (15–20 μm), some of which were contained deformation twins. This typical bimodal microstructure can largely increase the ductility of many metals and alloys [29]. During plastic deformation, the fine grains exhibited large microstrain than the coarse grains due to GBs effect, as shown in Fig. 7(a). Also, Kernel average misorientation map (Fig. 7(c)) have proved that local strain in this bimodal microstructure are very ununiform. Fine grains are suffered larger local misorientation, which introduced by high density of dislocation tangle structures, see in Fig. 7(f). When the overall uniform elongation increasing, these coarse grains accommodate the local strains and accumulate the large numbers of low angle GBs (Fig. 7(f)). Afterwards, the bimodal microstructures of AZ31 samples exhibits the largest ductility among grain refinement samples. In the other side, the samples with average grain size of 3, 6 μm shows relatively uniform grain size distribution, and

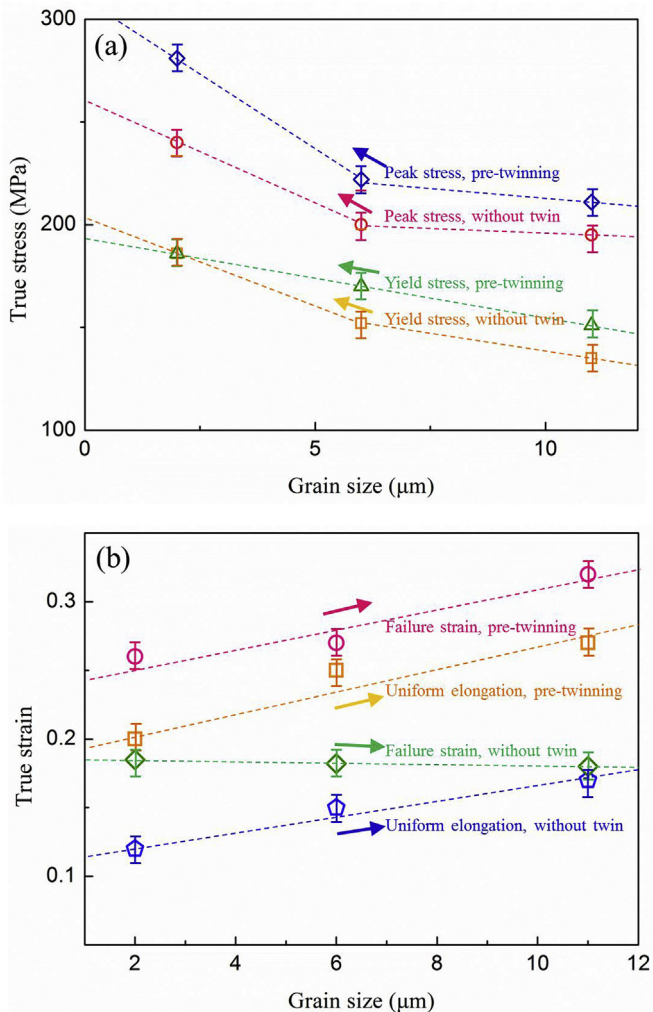


Fig. 8. Grain size and pre-twinning effect on (a) strength and (b) tensile ductility of AZ31 alloy at room temperature.

larger local misorientation concentrated around GBs, which finally result in crack nucleation and reduce the ductility, as seen in Fig. 7(b), (d) and (e).

Fig. 3 shows the microstructure evolution of fine grained AZ31 Mg alloy after dynamic compression. The twin boundary density increase (from 3% to 6%) with decreasing of grain size (from 11  $\mu\text{m}$  to 3  $\mu\text{m}$ ), which detected by EBSD method. Several studies have been investigated the contributions of grain size to the twin density of Mg alloy and suggest that the deformation twinning nucleation stress is more sensitive to the grain size than dislocation slip stress [30–32]. Our work also prove that macroscopic plastic deformation needs a greater twin number density in fine grained Mg alloy, which exhibited high yield strength.

#### 4.2. The effect of deformation twins on tensile deformation behavior

Recently, increasing investigates suggest that high  $\{10\bar{1}2\}$  extension twin density can effectively enhance yield strength of AZ31 without any compromise of ductility [33]. Xin et al. have reported that the  $\{10\bar{1}2\}$  extension twin can greatly enhance the formability of Mg alloy during hot rolling [34]. In this study, after grain refinement and pre-twinning through ECAP and dynamic compression, the strength and ductility are both largely improved,

as seen in Fig. 8(a), (b). The presence of a large number of  $\{10\bar{1}2\}$  extension twins in dynamic compressed samples was also confirmed by microstructure characterizations in Fig. 9. This indicates that high  $\{10\bar{1}2\}$  extension twin density changes the main deformation mode in subsequent tensile deformation. Fig. 9(a), (b) show that deformation twin density is higher in AZ31 samples with smaller grain size. And, it is well known that CRSS of basal slip and  $\{10\bar{1}2\}$  extension twin are very low in Mg alloy. So, the high twin density offers more dislocation nucleation sites and dislocation slip planes, which can contribute to tensile ductility improvement, see in Fig. 9(c), (d).

As we mentioned before, although non-basal slips are detected in some grains, basal slip and  $\{10\bar{1}2\}$  extension twins in a large number of grains determine the strength and ductility of the pre-twinning AZ31 samples at room temperature. Based on our study, it is accepted that three main mechanisms are suspected to contribute the enhancement of both strength and ductility in fine grained and pre-twinning samples [35]: (i) a Hall-Petch-like effect that arises from refinement GBs, (ii) the high density TBs impede the dislocation motion and multiplication, and (iii) change the crystal lattice to harder orientation. Of course, the mechanism (iii) only works as that detwinning transforms the twins in to the matrix, the matrix can be defined as a hard orientations structure. For mechanism (i) and (ii), the Kernel average misorientation maps (Fig. 9(a), (b)) and TEM images (Fig. 9(a), (b)) confirm that high density dislocation structures and dislocation nucleation occurred in and around GBs and TBs, which indicate that TBs not only acted as dislocation nucleation sites but also as barriers for dislocation motion. Thus, the ECAP and dynamic compression provides the capability of simultaneously achieving both high strength and ductility in the AZ31 alloy and our works demonstrate a considerable potential for using grain refinement and pre-twinning for the mechanical behavior development of Mg alloy.

#### 4.3. The effect of microstructure on failure mode

Fig. 10 depicts the fracture surface of AZ31 specimens with different microstructure. The fracture surface of as-received CG specimens shows a obvious major fracture edge and very few local dimples, which imply the low ductility and a mixed ductile and brittle fracture, as shown in Fig. 10(a). Fig. 10(b) shows the fracture surface of fine grained AZ31 specimens with average grain size of 3  $\mu\text{m}$ . After grain refinement, the dimples density increased, which indicated the enhancement of ductility compared with CG AZ31 alloy. In contrast, in fine grained and pre-twinning specimens the number of dimples was more than fine grained samples. And the distribution of dimples was very uniform, as seen in Fig. 10(c), (d). Moreover, the dimples in pre-twinning samples were deeper than those fine grained samples. These typical fracture surfaces are believed to be the evidence of good ductility after dynamic-compression. Therefore, it is supposed that tensile elongation of AZ31 alloy is promoted by the grain refinement and pre-twinning.

## 5. Conclusions

In summary, the present work demonstrates that grain refinement and pre-twinning at room temperature can improve the both strength and ductility in AZ31 Mg alloy. The high density of deformation twins was introduced in AZ31 Mg alloy by dynamic compression and the twin structure was well retained during tension tests. During plastic deformation, high density GBs and TBs can act as barriers for dislocation motion, which increase the strength of AZ31 Mg alloy. In another side, the TBs also displayed dislocation nucleation sites and provided new slip planes, which

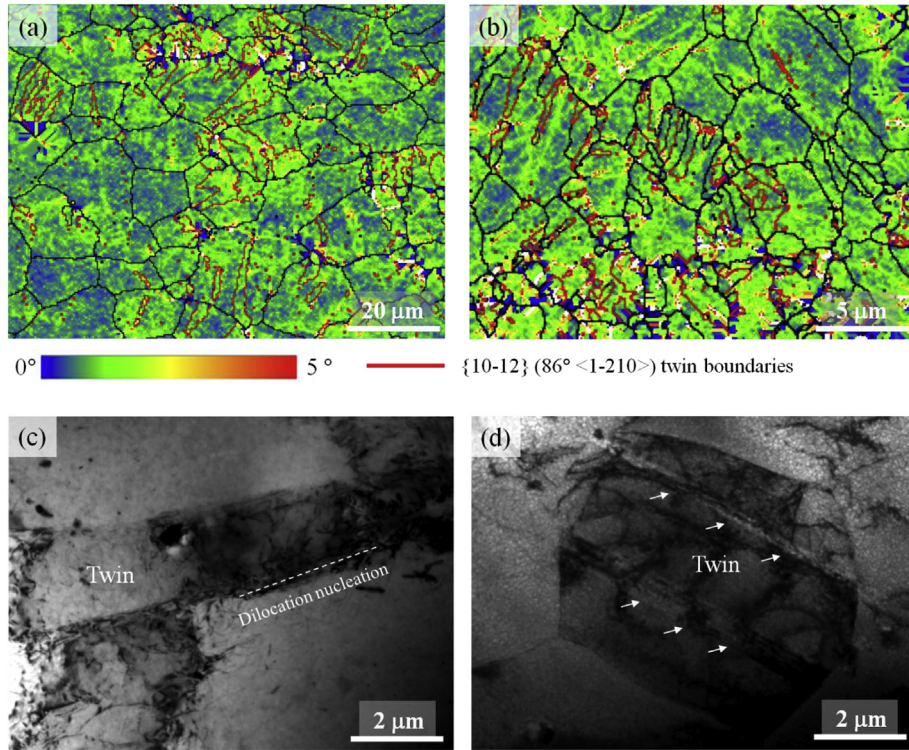


Fig. 9. Kernel average misorientation maps and TEM images show the pre-twinning effect on bimodal microstructures (a), (c) and fine grained microstructure (b), (d) of AZ31 alloy at room temperature.

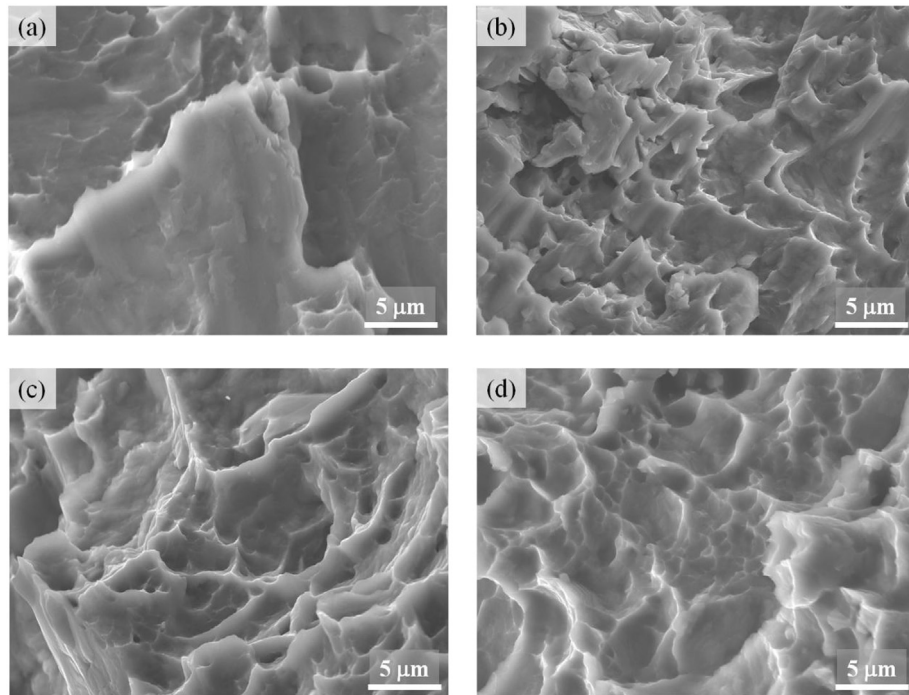
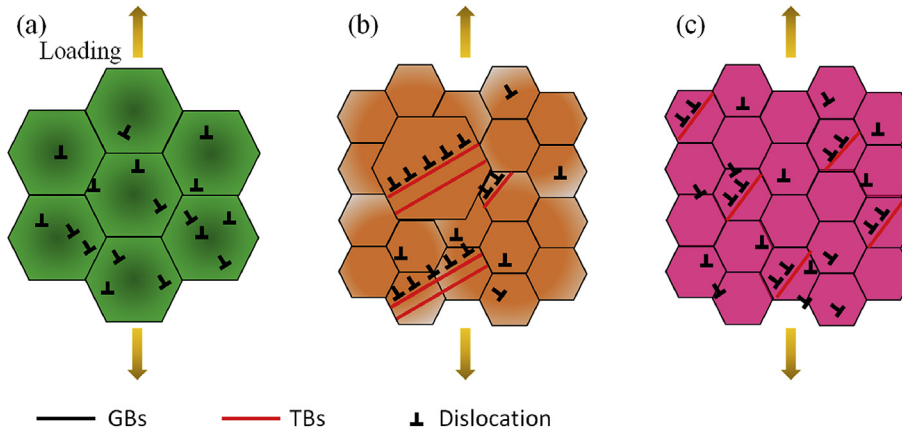


Fig. 10. Typical tensile fracture morphologies of AZ31 samples observed by SEM: (a) as-cast; (b) 4pass ECAPed; (c) 4pass ECAPed and pretwinning; (d) 8pass ECAPed and pretwinning.

contributed to the large ductility.

As shown in Fig. 11(a), the dislocation multiplication and motion in basal plane are the major deformation mode for CG AZ31 alloys. Under quasi-static loading, the micro-strain distribution is not

uniform, which largely depends on the initial crystallographic misorientation and defects density in deformed regions. After the deformed grains are strengthened by increasing dislocation density, the local plastic strain continued occurs in another grains,



**Fig. 11.** Diagram illustrating the microstructures effect on deformation mechanism of (a) CG; (b) bimodal grain distribution and pretwining; and (c) fine grained and pretwining AZ31 alloys during tensile tests.

which exhibit low dislocation density. During quasi-static plastic deformation, the strain hardening properties are major governed by the dislocation multiplication and interaction in limited basal  $\langle a \rangle$  slip plane.

After grain refinement and introducing high  $\{10\bar{1}2\}$  extension twin density by using ECAP and dynamic compression method in AZ31 samples, the deformation mode is significantly changed, as shown in Fig. 11(b) and (c). The twin density seen in the fine grained samples are considerably higher than in the coarse grained samples, because high yield strength for fine grained samples requires a greater twin density. The high density of deformation twins can act as new dislocation nucleation sites and provide more slip planes for dislocation motion, which reducing the local stress concentration and improve the plasticity of AZ31 alloys. Also, twinning controls the macroscopic strength of AZ31 alloy within bimodal and fine grained structure. Most of the strengthening effect is attributable to the high GB and TB density.

### Acknowledgement

We gratefully acknowledge financial support from National Natural Science Foundation of China (grant no. 11672254).

### References

- [1] B. Hutchinson, M.R. Barnett, A. Ghaderi, P. Cizek, I. Sabirov, Deformation modes and anisotropy in magnesium alloy AZ31, *Int. J. Mater. Res.* 100 (2009) 556–563.
- [2] T.M. Pollock, Weight loss with magnesium alloys, *Science* 328 (2010) 986–987.
- [3] W.J. Joost, P.E. Krajewski, Towards magnesium alloys for high-volume automotive applications, *Scripta Mater.* 128 (2017) 107–112.
- [4] M.H. Yoo, Slip, twinning, and fracture in hexagonal close-packed metals, *Metall. Trans. A* 12 (1981) 409–418.
- [5] M.R. Barnett, Twinning and the ductility of magnesium alloys: part I: “tension” twins, *Mater. Sci. Eng. A* 464 (2007) 1–7.
- [6] B. Clausen, C.N. Tome, D.W. Brown, S.R. Agnew, Reorientation and stress relaxation due to twinning: modeling and experimental characterization for Mg, *Acta Mater.* 56 (2008) 2456–2468.
- [7] Z. Wu, W.A. Curtin, The origins of high hardening and low ductility in magnesium, *Nature* 526 (2015) 62–67.
- [8] S.R. Agnew, O. Duygulu, Plastic anisotropy and the role of non-basal slip in magnesium alloy AZ31B, *Int. J. Plast.* 21 (2005) 1161–1193.
- [9] H. Somekawa, T. Mukai, Hall-Petch breakdown in fine-grained pure magnesium at low strain rates, *Metall. Mater. Trans. A* 46 (2015) 894–902.
- [10] W.T. Jia, F.K. Ning, Y.P. Ding, Q.C. Le, Y. Tang, J.Z. Cui, Role of pre-width reduction in deformation behavior of AZ31B alloy during break-down rolling and finish rolling, *Mater. Sci. Eng. A* 720 (2018) 11–23.
- [11] W.J. Kim, H.T. Jeong, Grain-size strengthening in equal channel angular pressing processed AZ31 Mg alloys with a constant texture, *Mater. Trans.* 46 (2005) 251–258.
- [12] W.J. Kim, S.I. Hong, Y.S. Kim, S.H. Min, H.T. Jeong, J.D. Lee, Texture development and its effect on mechanical properties of an AZ61 Mg alloy fabricated by equal channel angular pressing, *Acta Mater.* 51 (2003) 3293–3307.
- [13] J. Koike, T. Kobayashi, T. Mukai, H. Watanabe, M. Suzuki, K. Maruyama, K. Higashi, The activity of non-basal slip systems and dynamic recovery at room temperature in fine-grained AZ31B magnesium alloys, *Acta Mater.* 51 (2003) 2055–2065.
- [14] T. Mukai, M. Yamanoi, H. Watanabe, K. Higashi, Ductility enhancement in AZ31 magnesium alloy by controlling its grain structure, *Scripta Mater.* 45 (2001) 89–94.
- [15] S.M. Fatemi-Varzaneh, A. Zarei-Hanzaki, Accumulative back extrusion (ABE) processing as a novel bulk deformation method, *Mater. Sci. Eng. A* 504 (2009) 104–106.
- [16] Z.R. Zeng, J.F. Nie, S.W. Xu, C.H.J. Davies, N. Birbilis, Super-formable pure magnesium at room temperature, *Nat. Commun.* 8 (2017) 972.
- [17] B. Wang, L. Deng, N. Guo, Z. Xu, Q. Li, EBSD analysis of  $\{10\bar{1}2\}$  twinning activity in Mg-3Al-1Zn alloy during compression, *Mater. Char.* 98 (2014) 180–185.
- [18] A. Jain, S.R. Agnew, Modeling the temperature dependent effect of twinning on the behavior of magnesium alloy AZ31B sheet, *Mater. Sci. Eng. A* 462 (2007) 29–36.
- [19] H. Wang, C.J. Boehlert, Q.D. Wang, D.D. Yin, W.J. Ding, In-situ analysis of the tensile deformation modes and anisotropy of extruded Mg-10Gd-3Y-0.5Zr (wt%) at elevated temperatures, *Int. J. Plast.* 84 (2016) 255–276.
- [20] R.B. Figueiredo, Z. Szaraz, Z. Trojanova, P. Lukac, T.G. Langdon, Significance of twinning in the anisotropic behavior of a magnesium alloy processed by equal-channel angular pressing, *Scripta Mater.* 63 (2010) 504–507.
- [21] R.W. Armstrong, P.J. Worthington, A constitutive relation for deformation twinning in body centered cubic metals, in: R.W. Rohde, B.M. Butcher, J.R. Holland, C.H. Karnes (Eds.), *Metallurgical Effects at High Strain Rates*, Plenum Press, New York, 1973, p. 401.
- [22] V.M. Segal, Materials processing by simple shear, *Mater. Sci. Eng. A* 197 (1995) 157–164.
- [23] R.Z. Valiev, T.G. Langdon, Principles of equal-channel angular pressing as a processing tool for grain refinement, *Prog. Mater. Sci.* 51 (2006) 881–981.
- [24] G. Wan, B. Wu, Y.D. Zhang, G.Y. Sha, C. Esling, Anisotropy of dynamic behavior of extruded AZ31 magnesium alloy, *Mater. Sci. Eng. A* 527 (2010) 2915–2924.
- [25] J. Koike, R. Ohyama, Geometrical criterion for the activation of prismatic slip in AZ61 Mg alloy sheets deformed at room temperature, *Acta Mater.* 53 (2005) 1963–1972.
- [26] S. Choi, D.H. Kim, H. Lee, B.S. Seong, K. Piao, R.H. Wagoner, Evolution of the deformation texture and yield locus shape in an AZ31 Mg alloy sheet under uniaxial loading, *Mater. Sci. Eng. A* 526 (2009) 38–49.
- [27] F. Zhao, L. Wang, D. Fan, B.X. Bie, X.M. Zhou, T. Suo, Y.L. Li, M.W. Chen, C.L. Liu, M.L. Qi, M.H. Zhu, S.N. Luo, Macrodeformation twins in single-crystal aluminum, *Phys. Rev. Lett.* 116 (2016), 075501.
- [28] W.J. Kim, S.I. Hong, Y.S. Kim, S.H. Min, H.T. Jeong, J.D. Lee, Texture development and its effect on mechanical properties of an AZ61 Mg alloy fabricated by equal channel angular pressing, *Acta Mater.* 51 (11) (2003) 3293–3307.
- [29] Y.M. Wang, M.W. Chen, F.H. Zhou, E. Ma, High tensile ductility in a nano-structured metal, *Science* 419 (2002) 912–914.
- [30] F. Siska, L. Stratil, J. Cizek, A. Ghaderi, M.R. Barnett, Numerical analysis of twin thickening process in magnesium alloys, *Acta Mater.* 124 (2017) 9–16.
- [31] A. Ghaderi, M.R. Barnett, Sensitivity of deformation twinning to grain size in titanium and magnesium, *Acta Mater.* 59 (2011) 7824–7839.
- [32] L. Balogh, R.B. Figueiredo, T. Ungár, T.G. Langdon, The contributions of grain size, dislocation density and twinning to the strength of a magnesium alloy processed by ECAP, *Mater. Sci. Eng. A* 528 (2010) 533–538.
- [33] Y. Xin, M. Wang, Z. Zeng, M. Nie, Q. Liu, Strengthening and toughening of

- magnesium alloy by  $\{1\ 0\ -1\ 2\}$  extension twins, *Scripta. Mater.* 66 (2012) 25–28.
- [34] Y. Xin, M. Wang, Z. Zeng, G. Huang, Q. Liu, Tailoring the texture of magnesium alloy by twinning deformation to improve the rolling capability, *Scripta Mater.* 64 (2011) 986–989.
- [35] M. Knezevic, A. Levinson, R. Harris, R.K. Mishra, R.D. Doherty, S.R. Kalidindi, Deformation twinning in AZ31: influence on strain hardening and texture evolution, *Acta Mater.* 58 (2010) 6230–6242.